AIP | Applied Physics Letters

A light-driven turbine-like micro-rotor and study on its light-to-mechanical power conversion efficiency

Xiao-Feng Lin, Guo-Qing Hu, Qi-Dai Chen, Li-Gang Niu, Qi-Song Li et al.

Citation: Appl. Phys. Lett. **101**, 113901 (2012); doi: 10.1063/1.4751464
View online: http://dx.doi.org/10.1063/1.4751464
View Table of Contents: http://apl.aip.org/resource/1/APPLAB/v101/i11
Published by the American Institute of Physics.

Related Articles

Nonlinear output properties of cantilever driving low frequency piezoelectric energy harvester
Appl. Phys. Lett. 101, 223503 (2012)

A review on frequency tuning methods for piezoelectric energy harvesting systems
J. Renewable Sustainable Energy 4, 062703 (2012)

Effects of ocean thermal energy conversion systems on near and far field seawater properties—A case study for Hawaii
J. Renewable Sustainable Energy 4, 063104 (2012)

Limit on converted power in resonant electrostatic vibration energy harvesters
Appl. Phys. Lett. 101, 173904 (2012)

Metamaterial particles for electromagnetic energy harvesting
Appl. Phys. Lett. 101, 173903 (2012)

Additional information on Appl. Phys. Lett.

Journal Homepage: http://apl.aip.org/
Journal Information: http://apl.aip.org/about/about_the_journal
Top downloads: http://apl.aip.org/features/most_downloaded
Information for Authors: http://apl.aip.org/authors

ADVERTISEMENT

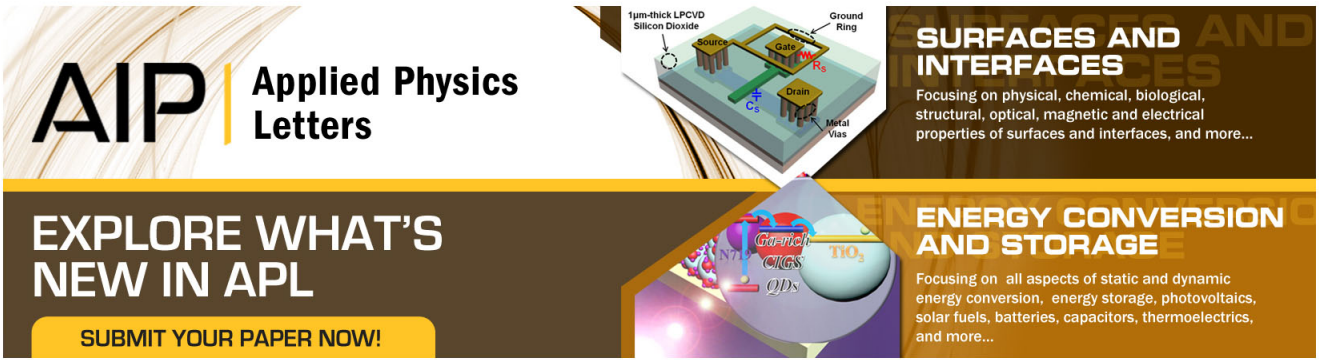

A light-driven turbine-like micro-rotor and study on its light-to-mechanical power conversion efficiency

Xiao-Feng Lin,[1] Guo-Qing Hu,[2] Qi-Dai Chen,[1,3,a)] Li-Gang Niu,[1] Qi-Song Li,[3] Andreas Ostendorf,[4] and Hong-Bo Sun[1,3,a)]
[1]*State Key Laboratory on Integrated Optoelectronics, College of Electronic Science and Engineering, Jilin University, Changchun 130012, China*
[2]*LNM, Institute of Mechanics, CAS, Beijing 100190, China*
[3]*College of Physics, Jilin University, Changchun 130012, China*
[4]*Ruhr University Bochum, Bochum 44721, Germany*

(Received 15 April 2012; accepted 24 August 2012; published online 11 September 2012)

A light driven micro-rotor is a useful telecontrolled device free of mechanical contact for power supply. However, low efficiency in converting light to mechanical power detracts from its advantages because it incurs a high power consumption that might result in unwanted effects. For a systematic study on conversion efficiency, we designed a turbine-like micro-rotor and made a quantitative analysis by computational fluid dynamics and semiclassical optics. Much larger in size than those ever reported, our rotor could rotate at over 500 r/min. Denoted by average angular momentum transfer, its conversion efficiency was experimentally determined as high as 34.55 $\hbar$/photon. © *2012 American Institute of Physics*. [http://dx.doi.org/10.1063/1.4751464]

Converting light power to mechanical power via no intermediate form, e.g., electricity or heat, has always been of great interest since immediate conversion generally means less dissipation and less complexity of system configuration. In the macroscale, it is usually difficult to realize such conversion due to an inefficient mechanism of photo-mechanical power conversion, which entails an enormous amount of light power. Nevertheless, inertia and resistance, which are commonly proportional to dimension cubed or squared, are much smaller in the microscale, where light can be directly used for trapping, translating, and rotating micro-objects.[1] The obvious advantage lies in the flexible control due to the absence of complex mechanics that transfers driving power. By contrast, electrorotation, another approach to rotate micro-particles, requires a set of closely arranged electrodes to generate a rotating electric field; therefore, the complexity of the system is highly increased and thus limits its application. A number of studies have been made on the optical manipulation of micro-rotors and have demonstrated great value of light-driven rotors in many fields such as micro-electro-mechanical system (MEMS),[2] microfluidic systems,[3] microrheology, medicine,[4] etc. In 2004, Bishop *et al.*[5] developed an optical system that can accurately measure the optical torque exerted on a rotating birefringent particle, which allows quantitative measurement of the viscosity and surface effects of liquid. In 2006, Leach *et al.*[6] reported a micropump consisting of two vaterite particles, which was controlled by optical tweezers and demonstrated good performance of fluid pumping and high flexibility of manipulation over the sense and speed of rotation. There are three major mechanisms for optical manipulation of micro-rotors: (i) The rotor is grabbed on certain points by one or several optical traps and rotates as the traps do,[7] but this requires an additional laser scanner and probably a beam splitter, which both increase the complexity of the whole system. (ii) The driving light carrying spin or orbital angular momentum exerts a torque on the rotor to cause rotation.[8,9] Although this approach is the most commonly used whereby small particles can attain rotation speeds of several hundred Hertz, it has limitations on the material or driving light of the rotor. For example, if circularly polarized light, which carries spin angular momentum, is adopted, the rotor should be made of absorptive or birefringence material, or be created form-birefringent; moreover, there is an upper bound on how much angular momentum each photon can transfer, which is 2 $\hbar$/photon. (iii) The torque that drives the rotor originates from the reflection, refraction, scattering of light,[10] or other interaction with matter,[11] rather than from the angular momentum that the driving light carries in itself, so one can make specific designs in which the deflection of the driving light is optimized in order to generate as much reaction force as possible. Be it any of the three mechanisms being adopted, light-driven micro-rotors that have been reported so far are generally less than 20 μm in size[12–15] because of low light torque efficiency resulting from rough, inappropriate designs. Intuitively, small size implies low resistance and high speed of rotation, but large size brings sufficient mechanical power and a wide effective range, when, for example, a micro-rotor is used as a mixer or a pump. However, large size rotors, which probably have to meet high resistance, need deliberate design, rather than merely copying macro-objects like gears, propellers, etc., to ensure that light can be converted into kinetic energy in high efficiency, thereby a low power input is sufficient and thus some unwanted effects such as heat damage can be avoided. Unfortunately, current designs of micro-rotors generally do not engender an effective conversion from light to mechanical energy with the angular momentum each photon contributes to the rotor being averagely lower than 2 $\hbar$/photon. In this letter, we report a turbine-like micro-rotor derived from a spiral phase plate[16] (SPP) that can generate a helical

a)Authors to whom correspondence should be addressed. Electronic mail: chenqd@jlu.edu.cn and hbsun@jlu.edu.cn.

wave.[17] As large as tens of microns, this micro-rotor could still rotate as fast as over 500 revolutions per minute (rpm) under a driving power less than 200 mW, which implies a high power conversion efficiency. Denoted by average angular momentum transfer, its ability to convert light to driving torque was quantitative analyzed by computational fluid dynamics (CFD) calculation and semiclassical optics and was experimentally determined as high as 34.55 $\hbar$/photon, much higher than that of those ever reported.

As a plane wave passes through a SPP, it is converted into a helical wave [Fig. 1(a)], which carries orbital angular momentum. At the same time, it gives the SPP an inverse angular momentum, exerting a torque that might actuate a rotation of the SPP if without restraint. To design a SPP rotor, we scale the SPP in azimuth from 2π to 2π/N (N is an integer greater than one) to make one blade [step 1, Fig. 1(b)] and then combine N blades to form a symmetric rotor body (step 2). To lessen any possible friction between the bottom of the rotor and any other surface and to prevent the rotor from flipping over in an optical trap, a shaft is fixed to the rotor along the axis (step 3). At last, a cylindrical well is built up around the rotor to prevent floating impurities from gathering to the optical trap (step 4).

We employed the femtosecond laser micro-fabrication technology[18] to realize the design of the rotor. A photoresist using methyl methacrylate as monomer was adopted as the material from which the rotor would be created. After fabrication, we used acetone to remove the unpolymerized resist so as to release the rotor made of poly(methyl methacrylate). The scanning electron microscopy (SEM) image of the rotor is shown as Fig. 1(c). The released rotor was then trapped and rotated in acetone by a linearly polarized laser from a semiconductor laser with a wavelength of 810 nm focused by a 40× objective lens. From the particle view of light, the rotation is caused by the reaction force of deflecting the photons [Fig. 1(d)], so there is no requirement on the polarization of driving light, i.e., it is unnecessary for the light to carry angular momentum *per se*. The movie of rotation—of a rotor with 30 blades and a 20-μm radius—recorded by a charge-coupled device (CCD) camera can be accessed through Ref. 19. By analyzing the playback recorded by a high-speed camera (Ref. 19, movie of a rotor with 15 blades and a 15-μm radius, note that the real motion is 60 times faster), we were able to figure out the speed of rotation.

Since the intensity of a focused laser varies with the distance away from the objective lens, it is necessary to investigate the correlation between the speed of rotation and the position of the focus plane. The results are shown in Fig. 2(a). When the focus plane was below the rotor, the gradient force of the optical trap pulled the rotor down against the substrate, as a result, combined with a concomitantly increased friction, it was difficult for the rotor to change its pose from leaning to standing [Fig. 2(b)]. When the focus plane had passed the gravity center of the rotor, the gradient force pulled it up from the substrate, so the rotor started standing up and rotating [Fig. 2(c)], as corresponds to the ascent stage of the fit curve. The speed of rotation reached the highest when the incident plane was as large as the cross section of the rotor body so that the helical slopes were made full use of converting light into driving torque and that the waste of light was least [Fig. 2(d)]. As the focus plane continued rising, the incident light decreased, which resulted in the decline of speed of rotation [Fig. 2(e)].

Besides the position of the focus plane, there are other three factors affecting speed of rotation, which are incident power, radius, and number of blades. As Figs. 3(a) and 3(b) show, regardless of radius or number of blades, all the correlations between speed of rotation and incident power indicate a linear dependence. The interpretation of the three factors pertaining to rotation involves further study on the hydrodynamics of the rotor, because resistance from the ambient fluid finally determines the upper limit of rotation speed when other parameters have been specified.

We employed the commercial CFD software FLUENT (ANSYS, Inc.) for the hydrodynamic computation. Shown in Fig. 4(a) is the filled contour, on the axial section, of velocity magnitude of the fluid field surrounding the rotating rotor with 15 blades and a diameter of 30 μm. Due to the odd number of blades, the axial section of the rotor is not symmetric. In addition to velocity contour, streamlines provide information about how the fluid circulates. As Fig. 4(b) shows, the green streamline starting from a point slightly above the blades depicts the

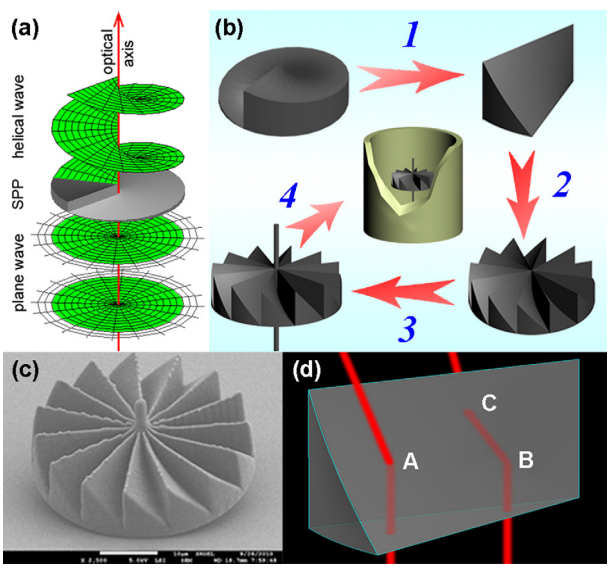

FIG. 1. (a) A SPP converting a plane wave into a helical wave. (b) Design of a turbine-like micro-rotor. (c) The SEM image of the fabricated one. (d) Schematic diagram of the driving mechanism: A – refraction on the helicoid; B – internal reflection on the helicoid; C – refraction on the vertical.

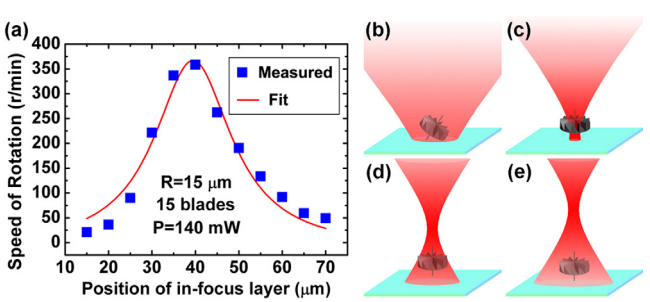

FIG. 2. (a) Correlation between speed of rotation and the position of in-focus plane. (b)–(e) Four typical positions of the focus plane off the substrate that result in different speeds of rotation.

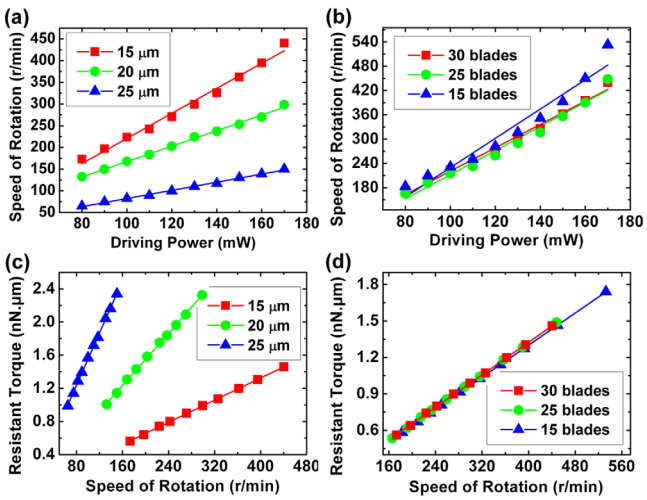

FIG. 3. Dependence of rotation speed upon driving power. (a) Comparison of 30-blade rotors with radius 15 μm, 20 μm, and 25 μm. (b) Comparison of 15-μm-radius rotors with 30, 25, and 15 blades. (c) and (d) Relations between rotation speed and driving torque, corresponding to (a) and (b), respectively.

flow in the region above the rotor; the red one indicates the flow surrounding the rotor; the blue one shows that the flow starting near the cylindrical wall extends downwards until gets close to the bottom, and then keeps spiraling inwards.

In addition to the kinematic information, CFD simulation also provided kinetic results needed by analysis of rotation. In a circumstance, as in our cases, where the fluid is Newtonian and incompressible with the Reynolds number far less than one, the Navier-Stokes equations, which describe the motion of fluid, can be reduced to

$$\begin{cases} \nabla p = \mu \nabla^2 \boldsymbol{u} + \boldsymbol{f} \\ \nabla \cdot \boldsymbol{u} = 0 \end{cases}, \tag{1}$$

where ∇p is the gradient of pressure, $\boldsymbol{u}$ is the velocity of the fluid, μ is the viscosity, and $\boldsymbol{f}$ is an external body force. ∇p represents the pressure force, $\mu \nabla^2 \boldsymbol{u}$ is the viscous force, and $\boldsymbol{f}$ is the gravity in our cases where it can be specified as $-\rho g z$, given ρ the density of the fluid, g the acceleration of gravity, and z the unit vector of the z axis. When cross-multiplied with $\boldsymbol{r}$, the distance vector between the axis and some point on the surface of the rotor, and then dot-multiplied with z, the first equation represents the relation of moments of the three forces

$$[\boldsymbol{r} \times (\nabla p)] \cdot z = [\boldsymbol{r} \times (\mu \nabla^2 u)] \cdot z + [\boldsymbol{r} \times (-\rho g z)] \cdot z, \tag{2}$$

where the third term is zero. As $|\boldsymbol{u}|$ is proportional to Ω the speed of rotation, the first and second terms as well as their sum representing the total resistant torque are proportional to Ω. As a result, the flow field shows a strictly linear correlation between resistant torque and rotation speed [Figs. 3(c) and 3(d)], as can be denoted by $T_r = k_T\, \Omega$, where k_T is the slope of the dependence curve and T_r is the resistant torque. The rate k_T, relating to the geometry of the rotor, reflects how much the shape affects the resistance. On the other hand, assuming the average angular momentum transfer (AAMT) from photons is q (in $\hbar$/photon), the driving torque from light can be given by

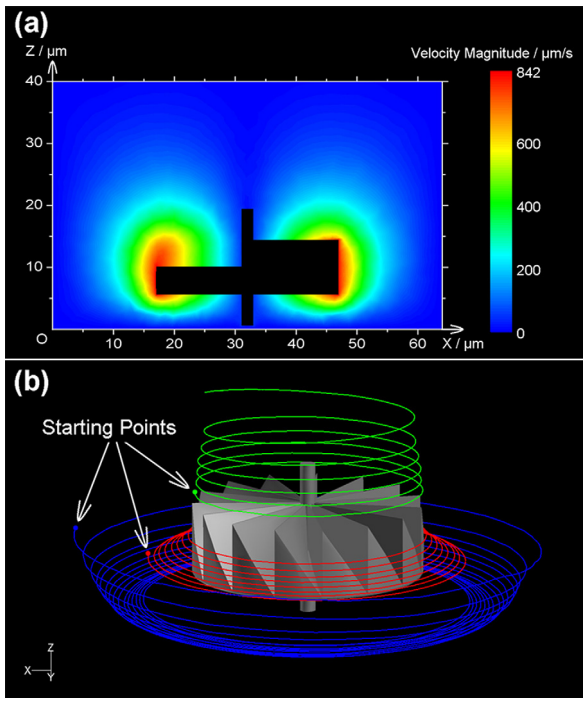

FIG. 4. (a) Contour of velocity magnitude in the plane y = 0 (15-blade rotor with radius 15 μm); (b) Streamlines shown by trajectories of massless, dimensionless virtual particles that start floating at different positions.

$$T_d = nq\hbar = \frac{P}{\hbar\omega} q\hbar = \frac{P}{\omega} q, \tag{3}$$

where n is the total number of the incident photons per unit time, P is the total power of the incident light, $\hbar$ is the reduced Planck constant, and ω is the angular frequency of the photons. When the rotation does not change with time, $T_d = T_r$, then we get

$$\Omega = \frac{qP}{\omega k_T} = k_p P, \tag{4}$$

where $k_p = q/(\omega k_T)$. This equation interprets the linearity of the correlation between Ω and P, as q and k_T are both constants only relating to the geometry. Given k_p and k_T, q can be calculated by $q = \omega k_P k_T$. It reflects essentially how much the shape affects the dynamic or, in other words, how efficiently the rotor utilizes the light for its rotation. Listed in Table I are the k_P, k_T, and AAMTs of five rotors for comparison. As mentioned above, the rotation of the rotor was activated and maintained by the optical torque derived from the light being refracted and internally reflected. From the particle view, light consists of photons, which carry momentum. When deflected, the photons impart momentum to the deflector according to the principle of momentum conservation; and if the deflections are distributed symmetrically around an axis, they result in a torque exerted on the deflector. To calculate this torque, and then the AAMT, we employed semiclassical method, which combines the particle view with ray tracing. Since the feature size of the helicoid-blade rotor is larger than the wavelength of the incident light, geometrical optics is still applicable. By ray tracing method, we calculated the momentum and exit point of the emergent photons that had entered the rotor per unit time through an infinitesimal area on the bottom so that the angular

TABLE I. Comparison of five micro-rotors.

Radius (μm)	Blades	k_P (rpm/mW)	k_T (nN·nm/rpm)	q[a] ($\hbar$/photon)
15	15	3.62	3.30	27.82/24.53
15	25	2.98	3.36	23.29/25.43
15	30	2.88	3.35	22.44/15.72
20	30	1.78	7.89	32.69/38.05
25	30	0.94	15.81	34.55/46.73

[a]Shown as "experimentally determined value/theoretically estimated value."

momentum per unit time, i.e., the torque, that these photons gave to the rotor could be calculated by cross-multiplying the distance vector (starting at and perpendicular to the axis and ending at the exit point) with the opposite of the change of momentum of the photons before going into and after coming out of the rotor within unit time. The total torque exerted on the rotor was the vector sum of all the cross-products. With the driving torque known, we were able to calculate the AAMT through Eq. (3). The results, shown in the last column of Table I, coincide with the experimental ones on the order of magnitude, and some of them are very close. The positive error, meaning the experimental result is greater than the theoretical one as in the cases of 15-μm-radius, 15-blade and 15-μm-radius, 30-blade rotors, may come from the overestimation of the resistance, which resulted from the decline of the viscosity. As the rotor was driven by focused laser, the enormous energy flux at the focus would probably cause an increase of temperature, even if the absorption rate of the liquid at this wavelength was neglectable in most cases. The viscosity of acetone correlates negatively with temperature, so the viscous torque as well as the total resistant torque and k_T in turn declined as the temperature increased. As a result, the overestimated k_T leads to an overestimated q, as $q = \omega k_P k_T$. The decline of the viscosity can also interpret the deviation from linearity at high powers discernable in the Ω-P charts as rotors would experience less resistance than without temperature increase. In addition, the k_T can be written as the product of the viscosity and a constant concerning the geometry of the rotor, i.e., $k_T = \mu k_g$. According to Eq. (4), the increment of rotation speed is then proportional to $1/k_g$, as $\Delta\Omega = qP/(\omega\Delta\mu k_g) \propto 1/k_g$. For the 15-blade rotor, the k_T, or more precisely the k_g, is comparatively smaller than that of the other two rotors, so the deviation is more obvious. As opposed to the positive error, the negative error, meaning the experimental result of q is less than the theoretical one, could be caused by overestimated driving power. The power was measured close to the exit pupil of the objective focusing the laser, so the actual power incident to the rotor was less since the laser had been partially reflected by the substrate. Some other factors, such as rounded edges of the blades, filled narrow gaps, etc., could also contribute to the deviation from the theoretical results. Besides the rotors whose data are demonstrated in Fig. 3 and Table I, we have also investigated rotors with fewer or more blades, e.g., 2, 5, 10, or 35 blades, and rotors with smaller radius, e.g., 10-μm radius, to find these rotors either hardly rotated or rotated in an unsteady way, e.g., with significant precession. Based on these investigations and the data in Table I, it can be concluded that when efficient utilization of light power, i.e., high q, is desirable, rotors should be designed with a large radius; when speed of rotation is emphasized, it is advisable to choose small radius to gain a large k_P; the number of blades does not have as significant influence on k_P, k_T, and q as the radius does, but too few or too many blades may result in low efficiency in light-mechanical power conversion—in the first case, the average slope of the blades is too gentle to adequately deflect the photons; in the second case, it is so steep that some photons may undergo several internal reflections and leave the rotor with a negative contribution of angular momentum—so that the rotation can be hardly activated or effectively maintained.

In summary, we reported a light driven turbine-like micro-rotor with AAMT up to 34.55 $\hbar$/photon, which shows high efficiency of the rotor converting light into driving torque, compared to those ever reported rotors. As a telecontrolled micro-device which might be applied to microfluidic systems, its performance has been examined and analyzed by CFD simulation and semiclassical optics. Compared to those of generally a few microns in diameter, the rotors have a much larger size of 30–50 μm, while their rotation speed could still reach up to 533 rpm and over if higher power had been available. The high conversion efficiency as well as flexibility of manipulation imparts a qualification to this micro-rotor as a competent micro-device for microfluidic purposes like mixing, pumping, and flow conducting and for other applications where efficient, large micro-rotors are needed.

The authors acknowledge the financial support from the Natural Science Foundation of China (NSFC) under Grants #90923037 and #61137001.

[1]A. Ashkin, Science **210**, 1081 (1980).
[2]S. T. Patton, W. D. Cowan, K. C. Eapen, and J. S. Zabinski, Tribol. Lett. **9**, 199 (2000).
[3]D. Spetzler, J. York, C. Dobbin, J. Martin, R. Ishmukhametov, L. Day, J. Yu, H. Kang, K. Porter, T. Hornung, and W. D. Frasch, Lab Chip **7**, 1633 (2007).
[4]D. L. Polla, A. G. Erdman, W. P. Robbins, D. T. Markus, J. Diaz-Diaz, R. Rizq, Y. Nam, H. T. Brickner, A. Wang, and P. Krulevitch, Annu. Rev. Biophys. **2**, 551 (2000).
[5]A. I. Bishop, T. A. Nieminen, N. R. Heckenberg, and H. Rubinsztein-Dunlop, Phys. Rev. Lett. **92**, 198104 (2004).
[6]J. Leach, H. Mushfique, R. di Leonardo, M. Padgett, and J. Cooper, Lab Chip **6**, 735 (2006).
[7]A. T. O'Neil and M. J. Padgett, Opt. Lett. **27**, 743 (2002).
[8]H. He, M. E. J. Friese, N. R. Heckenberg, and H. Rubinsztein-Dunlop, Phys. Rev. Lett. **75**, 826 (1995).
[9]M. E. J. Friese, T. A. Nieminen, N. R. Heckenberg, and H. Rubinsztein-Dunlop, Nature **394**, 348 (1998).
[10]S. Matsuo, S. Kiyama, Y. Shichijo, T. Tomita, S. Hashimoto, Y. Hosokawa, and H. Masuhara, Appl. Phys. Lett. **93**, 051107 (2008).
[11]M. Liu, T. Zentgraf, Y. Liu, G. Bartal, and X. Zhang, Nat. Nanotechnol. **5**, 570 (2010).
[12]P. Galajda and P. Ormos, Appl. Phys. Lett. **78**, 249 (2001).
[13]M. E. J. Friese and H. Rubinsztein-Dunlop, Appl. Phys. Lett. **78**, 547 (2001).
[14]P. Galajda and P. Ormos, Appl. Phys. Lett. **80**, 4653 (2002).
[15]S. Maruo, K. Ikuta, and H. Korogi, J. Microelectromech. Syst. **12**, 533 (2003).
[16]M. W. Beijersbergen, R. P. C. Coerwinkel, M. Kristensen, and J. P. Woerdman, Opt. Commun. **112**, 321 (1994).
[17]J. E. Curtis and D. G. Grier, Phys. Rev. Lett. **90**, 133901 (2003).
[18]S. Kawata, H. B. Sun, T. Tanaka, and K. Takada, Nature **412**, 697 (2001).
[19]See supplementary material at http://dx.doi.org/10.1063/1.4751464 for the movie of rotation recorded by a CCD and the movie of rotation recorded by a high-speed camera.